Earthquake Engineering, Tenth World Conference © 1992 Balkema, Rotterdam. ISBN 90 5410 060 5

Fluid-structure interaction analysis for spent fuel storage structures

C.-B. Yun, Y.-S. Kim & J.-M. Kim
Korea Advanced Institute of Science and Technology, Korea
J.-W. Kim, J.-M. Seo & Y.-S. Choun
Korea Atomic Energy Research Institute, Korea

ABSTRACT : In this paper, liquid sloshing effects in rectangular storage structures for spent fuel under earthquake loadings are investigated. Eulerian and Lagrangian approaches are presented. The Eulerian approach is carried out by solving the boundary value problem for the fluid motion. In the Lagrangian approach, the fluid as well as the storage structure are modelled by the finite element method. The fluid region is idealized by using fluid elements. The (1x1)-reduced integration is carried out for constructing the stiffness matrices of the fluid elements. Seismic analysis of the coupled system is carried out by the response spectra method. The numerical results indicate that the fluid forces on the wall obtained by two approaches are in good agreements. By including the effect of the flexibility of the wall, the forces due to fluid motion can be increased very significantly.

1 INTRODUCTION

The safety of the spent fuel storage structures is extremely important, because the failure of the structures, containing cooling water and spent fuel which are of high level in radioactivity, may have disastrous consequences on lives and environments. Seismic excitation is the most important force to be considered in the design of those structures. The objective of this study is to develop efficient methods for seismic analysis of the structures. The study focuses on the fluid-structure interactions including the effect of the wall flexibility of the structures.

There are two types of approaches for the solution of the coupled systems of the structure and fluid. One is the Eulerian approach, in which the fluid motion is formulated in terms of velocity potential : see Housner(1957), Veletsos(1974), Epstein (1976), Balendra(1982), Haroun(1983 , 1984) and Yun (1986). The other is the Lagrangian approach, in which the fluid may be treated as a solid with zero shear modulus : see Sundqvist(1983) and Chen(1990). In this study, both Eulerian and Lagrangian approaches are presented. The Eulerian approach is carried out by solving the boundary value problem for the fluid motion and applying Navier-Stokes equation for the hydrodynamic forces on the wall. In the Lagrangian approach, the storage structure and the contained fluid are modelled by the finite element method, utilizing a general purpose structural analysis program ADINA(1984). The fluid region is idealized by using the fluid elements. The gravity effect on the sloshing motion is represented by using a series of equivalent vertical springs along the free surface. The (1x1)-reduced integration is carried out for constructing the stiffness matrices of the fluid elements. Dynamic analysis of the coupled system is carried out for the earthquake loadings by the response spectra method.

The numerical results of several example cases indicate that the fluid forces on the wall obtained by two approaches are in good agreements. It has been also found that the effect of the flexibility of the wall is very important. By including the effect, the base shear and base moment of the structure can be increased very significantly.

2 EULERIAN APPROACH

2.1 *Modelling of the rectangular storage structures*

The storage structures are assumed to be rigidly mounted onto the bases on the ground and partially filled with fluid as shown in Figure 1. The behaviors of the structures during earthquake are basically 3-dimensional. However, for the computational simplicity, the 2-dimensional structure as shown in Figure 2 is considered in this study. The walls of the structures are modelled by using beam elements. The equivalent bending rigidity of the wall is determined in such a way that the fundamental natural frequency of the 3-dimensional structure may be maintained. In the actual analysis, only a half of the fluid-structure system is considered, because the motion of the system under horizontal earthquake loading is anti-symmetric with respect to the

vertical plane at the center.

2.2 *Velocity potential and hydrodynamic forces*

For the irrotational flow of an incompressible inviscid fluid, the velocity potential, $\phi(x,z;t)$, satisfies the Laplace equation in the fluid region.

$$\nabla^2\phi(x,z;t) = 0 \quad \text{in} \quad \Omega \tag{1}$$

Then, the fluid-wall boundary conditions can be expressed as follows:

$$\phi_{,x}(\pm L,z;t) = \dot{W}(z;t) \tag{2}$$

$$\phi_{,z}(x,0;t) = 0 \tag{3}$$

$$\phi_{,z}(x,H;t) = \dot{\xi}(x;t) \tag{4}$$

$$\rho\,\dot{\phi}(x,H;t) + \rho\,g\,\xi(x;t) = 0 \tag{5}$$

where $\xi(x;t)$ is the elevation of the free surface over the mean surface level; $W(z;t)$ is the horizontal displacement of the wall; $\phi_{,x}$ represents $\partial\phi/\partial x$; ρ is the mass density of fluid; and g is the acceleration of gravity.

The general solution for the Eq. (1), which satisfies the boundary condition on the tank wall, Eq. (2), can be expressed as,

$$\phi(x,z;t) = \sum_{n=1}^{\infty} A_n(z;t)\sin\lambda_n x + x\dot{W}(z;t) \tag{6}$$

where $\lambda_n = (2n-1)\pi/(2L)$ and $A_n(z;t)$ is the time varying coefficients of the n-th term in the sine series which is to be determined using the other boundary conditions. The free surface elevation can be also expressed in terms of the sine series as,

$$\xi(x;t) = \sum_{n=1}^{\infty}\eta_n(t)\ \sin\lambda_n x \tag{7}$$

where $\eta_n(t)$ represents the generalized free surface amplitude associated with $\sin\lambda_n x$.

Substituting Eqs. (6) and (7) into Eqs. (1), (3), (4) and (5), one can obtain expressions for $A_n(z;t)$ in terms of $\dot{W}(z;t)$ and $\eta_n(t)$. The horizontal displacement of the wall is represented by using third order polynomial of z within each beam element. Consequently, the deformation of the whole wall section is represented by much higher order terms. However, it is not practical to use the same interpolation functions to describe the fluid boundary condition along the wall, because the liquid motion is mostly associated with the low frequency vibration modes. Hence, an approximate shape which is *a third order polynomial function through the depth* of the contained liquid is used to obtain $A_n(z;t)$ in this study. The approximate shape, $\overline{W}(z;t)$, is determined by the least square fitting of the horizontal displacements of the beam at the nodes, $\{w(t)\}$, as follows,

$$W(z;t) \approx \overline{W}(z;t) = \{P(z)\}^T[R]\{w(t)\} \tag{8}$$

where $\{P(z)\}^T = < 1, z, z^2, z^3 >$ and the coefficient matrix $[R]$ can be obtained from the z-coordinates of the nodes below free surface.

Once the solution for $A_n(z;t)$ is obtained, the velocity potential can be expressed into two parts as,

$$\phi(x,z;t) = \phi_I(x,z;\{\dot{w}(t)\}) + \phi_C(x,z;\int_0^t\{\eta(\tau)\}d\tau) \tag{9}$$

where ϕ_I and ϕ_C may be considered as the impulsive and the convective components of the velocity potential, respectively.

Substituting Eq. (9) into the free surface boundary conditions, one can obtain the relationship between $\{\eta\}$ and $\{\ddot{w}\}$ as,

$$[M_{ff}]\{\ddot{\eta}\} + [K_{ff}]\{\eta\} = [S]\{\ddot{w}\} \tag{10}$$

where diagonal matrices $[M_{ff}]$ and $[K_{ff}]$ can be interpreted as mass and stiffness matrices associated

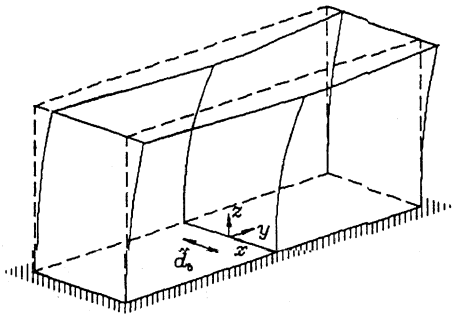

Figure 1. Rectangular storage structure.

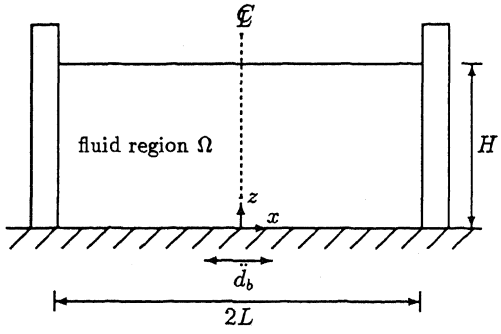

Figure 2. 2-dimensional model of a rectangular storage structure.

with the free surface motion; and $[S]$ is the coefficient matrix of the exciting force associated with the wall motion.

Using Eq. (9) and Navier-Stokes equation, the hydrodynamic pressure exerted on the wall can be expressed in terms of velocity potential. Then, using the virtual work principle, the nodal hydrodynamic force vector, $\{F\}$, can be obtained as,

$$\{F\} = -[M_a]\{\ddot{w}\} - [S]^T\{\eta\} \tag{11}$$

where $[M_a]$ is the hydrodynamic added mass matrix associated with the horizontal movement of the liquid; and $[S]$ is the matrix relating the horizontal force on the wall with the free surface motion. It can be easily shown that the matrix $[S]$ in Eqs. (10) and (11) are identical.

2.3 *Equation of motion of fluid-structure system*

Combining Eqs (10) and (11), the equation of the fluid-structure system can be obtained as,

$$\begin{bmatrix} M_{ss}+\bar{M}_a & 0 \\ -\bar{S} & M_{ff} \end{bmatrix} \begin{Bmatrix} \ddot{d} \\ \ddot{\eta} \end{Bmatrix} + \begin{bmatrix} K_{ss} & \bar{S}^T \\ 0 & K_{ff} \end{bmatrix} \begin{Bmatrix} d \\ \eta \end{Bmatrix} = \begin{Bmatrix} R_e \\ 0 \end{Bmatrix} \tag{12}$$

where $\{d\}$ is the nodal displacement vector of the wall; $\{R_e\}$ is the reaction vector at the base; $[\bar{M}_a]$ and $[\bar{S}]$ are the matrices corresponding to $[M_a]$ and $[S]$ but with proper dimensions. Decomposing the displacement vector $\{d\}$ into the components at the base $\{d_b\}$ and at the free nodes $\{d_w\}$, Eq. (12) can be rewritten as,

$$\begin{bmatrix} M_{bb} & M_{bw} & 0 \\ M_{wb} & M_{ww} & 0 \\ -\bar{S}_b & -\bar{S}_w & M_{ff} \end{bmatrix} \begin{Bmatrix} \ddot{d}_b \\ \ddot{d}_w \\ \ddot{\eta} \end{Bmatrix} + \begin{bmatrix} K_{bb} & K_{bw} & \bar{S}_b^T \\ M_{wb} & M_{ww} & \bar{S}_w^T \\ 0 & 0 & K_{ff} \end{bmatrix} \begin{Bmatrix} d_b \\ d_w \\ \eta \end{Bmatrix} = \begin{Bmatrix} R_e \\ 0 \\ 0 \end{Bmatrix} \tag{13}$$

From Eq. (13), it can be observed that the coefficient matrices are unsymmetric due to the presence of the matrix $[S]$ representing the coupling effect between the surface wave motion and the wall motion. Therefore the extraction of the eigenvalues and eigenvectors as well as the solution of the coupled equation becomes extremely difficult. Owing mainly to the difficulty, the coupling terms have been commonly omitted in many investigations: see Veletsos(1974) and Haroun(1983). In the present study, however, Eq. (13) is transformed by premultiplying a matrix $[T]$ as

$$\begin{bmatrix} M_{bb} & M_{bw} & 0 \\ K_{ww}M_{ww}^{-1}M_{wb} & K_{ww} & 0 \\ \bar{S}_wM_{ww}^{-1}M_{wb} - \bar{S}_b & 0 & M_{ff} \end{bmatrix} \begin{Bmatrix} \ddot{d}_b \\ \ddot{d}_w \\ \ddot{\eta} \end{Bmatrix} + \begin{bmatrix} K_{bb} & \bar{S}_b^T \\ K_{ww}M_{ww}^{-1}K_{ww} & K_{ww}M_{ww}^{-1}\bar{S}_w^T \\ \bar{S}_wM_{ww}^{-1}K_{ww} & K_{ff}+\bar{S}_wM_{ww}^{-1}\bar{S}_w^T \end{bmatrix} \begin{Bmatrix} d_b \\ d_w \\ \eta \end{Bmatrix} = \begin{Bmatrix} R_e \\ 0 \\ 0 \end{Bmatrix} \tag{14}$$

and

$$[T] = \begin{bmatrix} I & 0 & 0 \\ 0 & K_{ww}M_{ww}^{-1} & 0 \\ 0 & \bar{S}_wM_{ww}^{-1} & I \end{bmatrix} \tag{15}$$

By expressing the displacement vector of the free nodes, $\{d_w\}$, as the sum of the ground movement, $\{d_b\}$, and the relative displacement to the ground movement, $\{d_r\}$, i.e.,

$$\{d_w\} = [I, I, \cdots, I]^T\{d_b\} + \{d_r\} \tag{16}$$

the following equation with symmetric matrices can be obtained from the second and the third rows of Eq. (14),

$$\begin{bmatrix} K_{ww} & 0 \\ 0 & M_{ff} \end{bmatrix} \begin{Bmatrix} \ddot{d}_r \\ \ddot{\eta} \end{Bmatrix} + \begin{bmatrix} K_{ww}M_{ww}^{-1}K_{ww} & K_{ww}M_{ww}^{-1}\bar{S}_w^T \\ \bar{S}_wM_{ww}^{-1}K_{ww} & K_{ff}+\bar{S}_wM_{ww}^{-1}\bar{S}_w^T \end{bmatrix} \begin{Bmatrix} d_r \\ \eta \end{Bmatrix} = -[M_e]\{\ddot{d}_b\} \tag{17}$$

where $[M_e]$ is the effective mass matrix for the base movements as,

$$[M_e] = \begin{bmatrix} K_{ww}M_{ww}^{-1}K_{wb} + K_{ww}[I, I, \cdots, I]^T \\ \bar{S}_wM_{ww}^{-1}M_{wb} - \bar{S}_b \end{bmatrix} \tag{18}$$

From the Eq. (17), the natural frequencies and the mode shapes can be readily computed. Then, the seismic response of the fluid-structure system can be calculated by the response spectra method utilizing mode superposition.

3 LAGRANGIAN APPROACH

In this approach, the contained fluid as well as the storage structure are modelled by the finite element method. A general purpose structural analysis program ADINA is utilized for this analysis. As in the Eulerian approach described in the previous section, the fluid-structure interaction analysis is carried out by using 2-dimensional model. Plane strain conditions are assumed for the analysis against the horizontal earthquake excitations. The walls of the storage structure are modelled by using 4-noded solid elements. The fluid region is represented by utilizing 4-noded fluid elements.

The fluid elements used are equivalent to the solid elements with zero shear modulus but with an approximate bulk modulus for the compressibility of the contained fluid. The (1x1)-reduced integration is carried out for constructing stiffness matrices

of the fluid elements, since the (2x2)-normal integration of the 4-noded fluid elements causes overestimations of the stiffness of the fluid elements. The (1x1)-reduced integration gives constant pressure within an element and no stiffness against deformation shape without volume change. Consequently, spurious zero energy modes may be produced in the modal analysis. In this study, the spurious modes are identified based on the results of the modal analysis, and they are disregarded in the dynamic response analysis.

The effect of the restoring force on the free surface due to gravity, which is associated with Eq. (5), can be represented by a series of vertical equivalent springs. When a quiescent free surface is disturbed by a vertical displacement, ξ, the restoring forces, f, due to the pressure change and the stiffness of the corresponding equivalent spring, k, can be evaluated as

$$f = -\rho g \xi \, dS \tag{19}$$

$$k = f/\xi = -\rho g \, dS \tag{20}$$

where dS is an infinitesimal area of the free surface.

The relative motion of the fluid along the wall is allowed only in the tangential direction to the wall as shown in Figure 3.

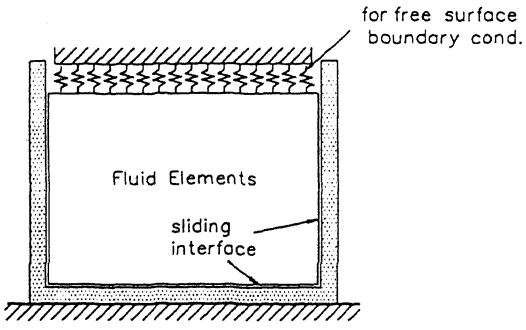

Figure 3. Finite element modelling for a flexible wall case.

4 NUMERICAL EXAMPLE AND DISCUSSIONS

4.1 *Properties of example cases*

Three cases of reinforced concrete structures for the storage of spent fuel are investigated. The widths of the structures(2L) are taken as 12, 30 and 60m, respectively. The wall thickness(h) is taken to be 1.2m for three structures. The fluid is assumed to be filled upto 13m above the base.

The material properties of the concrete storage structures are : Young's modulus(E)=19.6 GPa, Poisson's ratio(ν) =0.2 and mass density(ρ_s) =2.4× $10^3 Kg/m^3$. The properties of fluid elements are: bulk modulus(K) =2.0GPa, mass density(ρ)=1.0× $10^3 Kg/m^3$.

For the seismic response analysis, the design response spectrum for the horizontal direction recommended by US NRC Regulatory Guide 1.60 is used. The peak ground acceleration is taken as $0.2g$, and the modal damping ratio is 0.5 percent for each mode.

4.2 *Free vibration analysis*

For the seismic excitations in the horizontal direction, only the ant-isymmetric modes of the fluid sloshing and the structural motions contribute to the dynamic response. The frequencies of the anti-symmetric sloshing modes computed for three structures are listed in Table 1. Good agreements can be observed between the results by different approaches. It is also found that the effect of wall flexibility to the sloshing frequencies are negligible. The natural frequencies of the anti-symmetric structural modes are also evaluated. The added mass effect is included in the analysis. The first two frequencies are shown in Table 2. Fairly good agreements between the results by the Eulerian and Lagrangian approaches can be observed.

From the results of the Lagrangian approach utilizing the finite element idealization both for the structure and the fluid, the first 29 modes are found to be the sloshing modes. The first two antisymmet-

Table 1. Frequencies of anti-symmetric sloshing modes (Hz)

Width	Natural	Rigid wall			Flexible wall	
	Frequency	Eulerian	Lagrangian	Housner	Eulerian	Lagrangian
12m	ω_1	0.26	0.26	0.26	0.26	0.26
	ω_3	0.44	0.36	0.44	0.44	0.36
30m	ω_1	0.15	0.15	0.15	0.15	0.15
	ω_3	0.28	0.24	0.28	0.28	0.24
60m	ω_1	0.09	0.09	0.09	0.09	0.09
	ω_3	0.19	0.20	0.19	0.19	0.20

ric structural modes are the 31^{st} and 33^{rd} modes as shown in Figure 4. The corresponding natural frequencies are found to be 3.0 and 17.0 Hz for the structure of 30m wide. These values are slightly less than those(3.2 and 19.9 Hz) obtained by the Eulerian approach. The discrepancies may be caused by different ways of modelling the wall structures: i.e., beam elements in the Eulerian approach and plane strain elements in the Lagrangian approach.

Table 2. Frequencies of anti-symmetric structural modes. (Hz)

Width	Natural Frequency	Eulerian	Lagrangian
12m	ω_1^{str}	3.3	2.8
	ω_3^{str}	20.7	18.4
30m	ω_1^{str}	3.2	3.0
	ω_3^{str}	19.9	17.0
60m	ω_1^{str}	3.3	3.0
	ω_3^{str}	20.0	16.7

4.3 *Free surface elevation*

Table 3 shows the maximum free surface elevation obtained by the Eulerian and the Lagrangian approaches. Maximum elevation mainly depends on the first sloshing mode. The effect of the wall flexibility on the sloshing motion is found to be negligible. The results obtained by the Lagrangian approach are in good agreements with those by the Eulerian and the Housner's methods.

Table 3. Maximum free surface elevation (m)

Width	Eulerian	Lagrangian	Housner
12m	0.91 (0.91)	0.97 (0.96)	- (1.27)
30m	1.14 (1.13)	1.14 (1.13)	- (1.29)
60m	1.13 (1.13)	1.12 (1.12)	- (1.04)

Note : The values in the parentheses are obtained from rigid wall cases, the others from flexible wall cases.

4.4 *Base shear and base moment*

The maximum shear and bending moments hydrodynamically induced at the bases of the walls are evaluated, and the results are shown in Tables 4 - 5. Comparisons with the results by the Eulerian approach indicate that the convective components are evaluated fairly accurately by the Lagrangian approach, while the impulsive components seem to be underestimated, particularly for the cases with rigid walls. However, for the cases with flexible walls, the discrepancies are found to be less than 5 percent. It is noted that the maximum base shears and bending moments for the flexible wall cases are about 3 times greater than those for the rigid wall cases. It is because the fundamental natural frequencies of the wall structures are in the range, where the spectral accelerations of the input response spectrum are about 5 times of the maximum ground acceleration.

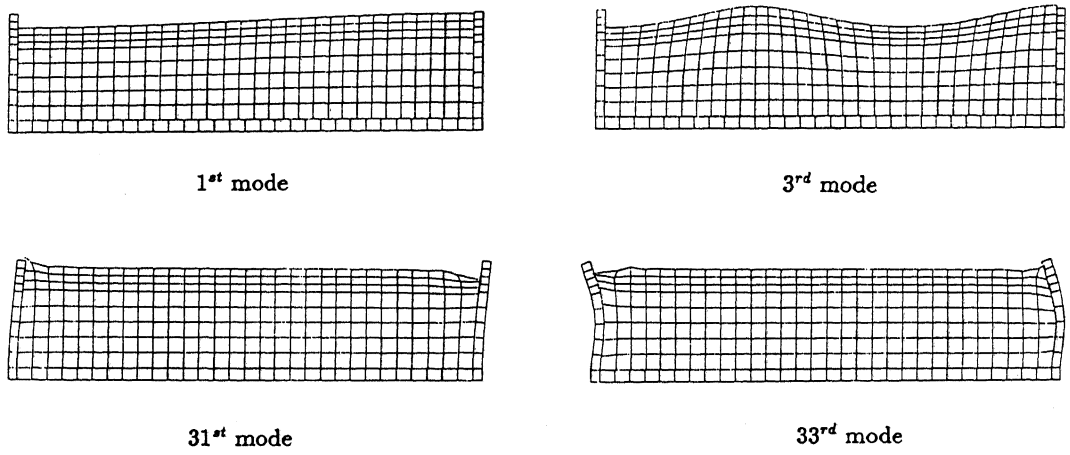

Figure 4. Anti-symmetric mode shapes for the shoshing and the structural modes of a flexible wall.

5 CONCLUSIONS

From the example analysis, it has been found that the Lagrangian approach utilizing the finite element modelling for the structure and the contained fluid yields very good results for the hydrodynamic forces on the wall, compared with those obtained by the more conventional Eulerian approach. Considering the versatility of the finite element modelling, the Lagrangian approach is judged to be a possible alternative way for the fluid-structure interaction analysis, particularly for the storage structures with complex geometries. It has been also found that the effects of the wall flexibility can be very important for the seismic analysis of the storage structures. By including these effects, the hydrodynamic forces on the wall may be amplified as much as three times of those corresponding to the rigid wall cases.

REFERENCES

ADINA Engineering AB, 1984. *ADINA User's Manual*, Sweden.

Balendra, T., Ang, K.K., Paramasivam, P. and Lee, S.L. 1982. Seismic design of flexible cylindrical liquid storage tanks. *Earthquake Engineering and Structural Dynamics 10*: 477-496.

Chen, H.C. and Taylor, R.L. 1990. Vibration analysis of fluid-solid system using a finite element displacement formulation. *Int. J. for Numerical Methods in Engineering 29*: 683-698.

Epstein, H.I. 1976. Seismic design of liquid storage tanks. *J. of Structural Division ASCE 102*: 1659-1673.

Haroun, M.A. 1983. Vibration studies and tests of liquid storage tanks. *Earthquake Engineering and Structural Dynamics 11*: 179-206.

Haroun, M.A. 1984. Stress analysis of rectangular walls under seismically induced hydrodynamic loads. *Bulletin of the Seismological Society of America 74*: 1031-1041.

Housner, J.W. 1957. Dynamic pressure on accelerated fluid container. *Bulletin of the Seismological Society of America 47*: 15-35.

Sundqvist, J. 1983. An application of ADINA to the solution of fluid-structure interaction problems. *Computers & Structures 17*: 793-807.

U.S. NRC Regulatory Guide 1.60. 1973. *Design response spectrum for nuclear power plants.*

Veletsos, A.S. 1974. Seismic effects in flexible liquid storage tanks. *Proc. Int. Assoc. for Earthquake Engineering 1*: 630-639.

Yun, C.B. and Lee, C.G. 1986. Liquid sloshing effect in flexible storage tanks. *Proc. 5th Congress Asian and Pacific Regional Division. Int. Assoc. for Hydraulic Research.*: 437-449.

Table 4. Maximum base shear forces (KN)

Width	Eulerian approach			Lagrangian approach			Housner method			
	Convec.	Impul.	SRSS	Convec.	Impul.	SRSS	Convec.	Impul.	SRSS	ABS
12m	33	359	361	31	354	355	-	-	-	-
	(33)	(112)	(117)	(31)	(99)	(104)	(33)	(127)	(131)	(161)
30m	90	543	551	90	527	535	-	-	-	-
	(90)	(164)	(187)	(89)	(127)	(156)	(90)	(187)	(208)	(277)
60m	120	546	559	117	518	531	-	-	-	-
	(120)	(165)	(204)	(117)	(106)	(158)	(109)	(195)	(223)	(304)

Note : The values in the parentheses are for the rigid wall cases, the others are for the flexible wall cases.

Table 5. Maximum base moments (KN-m)

Width	Eulerian approach			Lagrangian approach			Housner method			
	Convec.	Impul.	SRSS	Convec.	Impul.	SRSS	Convec.	Impul.	SRSS	ABS
12m	312	2522	2541	298	2497	2515	-	-	-	-
	(310)	(609)	(683)	(297)	(522)	(601)	(328)	(631)	(711)	(959)
30m	668	3425	3490	657	3324	3389	-	-	-	-
	(666)	(848)	(1078)	(655)	(663)	(932)	(694)	(925)	(1156)	(1619)
60m	810	3334	3431	783	3168	3263	-	-	-	-
	(810)	(844)	(1174)	(781)	(584)	(975)	(784)	(961)	(1241)	(1745)

Note : The values in the parentheses are for the rigid wall cases, the others are for the flexible wall cases.